

CrystEngComm

Accepted Manuscript



This is an *Accepted Manuscript*, which has been through the Royal Society of Chemistry peer review process and has been accepted for publication.

Accepted Manuscripts are published online shortly after acceptance, before technical editing, formatting and proof reading. Using this free service, authors can make their results available to the community, in citable form, before we publish the edited article. We will replace this *Accepted Manuscript* with the edited and formatted *Advance Article* as soon as it is available.

You can find more information about *Accepted Manuscripts* in the [Information for Authors](#).

Please note that technical editing may introduce minor changes to the text and/or graphics, which may alter content. The journal's standard [Terms & Conditions](#) and the [Ethical guidelines](#) still apply. In no event shall the Royal Society of Chemistry be held responsible for any errors or omissions in this *Accepted Manuscript* or any consequences arising from the use of any information it contains.



Hierarchical Architecture of WO₃ Nanosheets by Self-assembly of Nanorods for Photoelectrochemical Application

Tao Zhang, Jinzhan Su* and Liejin Guo*

Received 00th January 20xx,
Accepted 00th January 20xx

DOI: 10.1039/x0xx00000x

www.rsc.org/crystengcomm

We reported a facile solvothermal strategy for hierarchical architectures of WO₃ nanosheets with WO₃ nanorod branches standing orderly on nanosheets. An enhanced photoelectrochemical activity is achieved, attributable to the highly porosity provided by the hierarchical architecture. The novel 3D nanostructure holds great potentials in photocatalysis, concurrent filtration, water purification and chemical sensing.

1. Introduction

Photocatalytic technology based on semiconductor materials has been considered as an important route for energy conversion and water purification since the pioneer work on TiO₂.¹ Over the past two decades, various TiO₂ nano-architectures have been designed and used for photocatalysis, photovoltaics, water purification etc.²⁻⁷ Among the reported novel fabrications, the hierarchical assembly of nanocrystals with different dimensions are of great significance and have received extensive attention because of their desirable functionalities and great potential. For example, hierarchical nanostructures of ZnO, MnO₂, Fe₂O₃ and CeO₂, have been successfully prepared by different methodologies of solution based, template assisted and electrochemical synthesis method.⁸⁻¹¹

Different from TiO₂ absorbing only UV light, tungsten trioxide (WO₃) is regarded as one of the best candidates for visible light driven photocatalytic application. To date, WO₃-based hierarchical nanostructures have drawn much attention as a multifunctional material in a broader field. Flower-like and microsphere-like hierarchical WO₃ architectures have been designed and fabricated for ion storage, photocatalysis and gas sensing.¹²⁻¹⁵ Rod/wire-like hierarchical WO₃ architectures, such as coaxial nanowire heterojunctions,¹⁶ epitaxial heterostructures and homojunction¹⁷⁻¹⁸ were also reported for their applications in electrochromic devices, field-emission devices and photocatalysis.

Yet there are few reports on synthesis of sheet-like hierarchical architectures formed by assembly of 1D/2D

nanostructures. Zheng *et al.* have reported a solution-process synthesis of 2D TiO₂ nanosheets coated with well-aligned 1D ZnO nanorod arrays, which showed an enhanced PEC performance.¹⁹ Similar hierarchical of homogenous ZnO nanowire-nanosheet architectures have been fabricated by a two-step method combined electrodeposition with aqueous chemical growth by Xu *et al.*²⁰ In addition, hydrated tungsten trioxide with various hierarchical architectures including flakes architectures on conductive zinc substrate has been successfully fabricated by a zinc substrate-induced method.²¹ Self-assembly of K_xWO₃ nanosheet consisting of superfine nanowires was synthesized by Jia *et al.*²² via a vapor-solid mechanism in ambient air with W foil as W source. There is no doubt that direct fabrication of hierarchical structures on conductive substrates is gaining increasing attention.

Herein, we for the first time have synthesized a hierarchical self-assembly of WO₃ nanorod/nanosheet on the FTO substrate by a simple solvothermal growth and annealing route. The mechanism for formation of the 3D hydrated tungsten trioxide architectures was explored and the photoelectrochemical performance of the obtained hierarchical WO₃ was evaluated.

2. Experimental

2.1 Methods

Similar to our previous report²³, tungstic acid precursor solution was prepared by dissolving 2.5 g of H₂WO₄ into a mixed-solution containing 50 mL H₂O and 50 mL 30 wt % H₂O₂ and then heated at 98 °C in a water bath with stirring. The resulting clear solution was diluted using deionized water to 100 mL with a molar concentration of 0.1M. In a typical process, 2.0 mmol ammonium oxalates were dissolved into 50 mL mixed-solvent containing 30 mL ethanol and 20 mL deionized water under vigorous stirring; then the concentrated hydrochloric acid was applied to adjust the acidity of precursor

International Research Center for Renewable Energy, State Key Laboratory for Multiphase Flow in Power Engineering, Xi'an Jiaotong University, Xi'an 710049, P. R. China

E-mail: j.su@mail.xjtu.edu.cn, lj-guo@mail.xjtu.edu.cn.

Electronic Supplementary Information (ESI) available: some supplementary figures. See DOI: 10.1039/x0xx00000x

solution and 5ml prepared tungstic acid precursor with concentration of 0.1M as added to the reaction solution. After 30min's stirring, the obtained homogeneous solution was transferred into a Teflon-lined stainless steel autoclave. Subsequently, a FTO-glass substrate (coated with a WO_3 seed layer) was obliquely placed against on the inner wall of Teflon-lined and completely immersed in solution. Then, the Teflon-lined stainless steel autoclave was sealed and placed in an oven which was maintained at 200°C for 5h. After the autoclave was cooled down naturally to room temperature, the substrate was taken out and rinsed with deionized water and ethanol and then dried in air at room temperature. The as-prepared samples were further annealed at 400°C , 500°C or 600°C in air for 2h with a heating rate of $3.3^\circ\text{C}/\text{min}$ and the final obtained products were labeled as W400, W500 and W600, respectively.

2.2 Characterization

The morphological, structural and optical properties of the hierarchical $\text{WO}_3(\text{H}_2\text{O})_x$ and WO_3 films were characterized by X-ray diffraction technique (XRD, $\text{CuK}\alpha$, 40KV, 40mA, PANalytical Corp), scanning electron microscope (SEM, model JSM-7800F) and transmission electron microscope (TEM, FEI Tecnai G2 F30), UV-Vis spectrophotometer (HITACHI U-4100) and thermal analyzer (STA 449C). Photocurrent densities were measured by a CHI 760D scanning potentiostat (CH Instruments). The scanning rate was $10\text{mV}/\text{s}$, and the scanning direction was from low to high potential. A 500W xenon lamp coupled with an AM1.5 filter was used as the light source. The light intensity was set at $100\text{mW}/\text{cm}^2$. The photoelectrochemical testing system in this paper was examined using three-electrode cells (Pt/(Ag/AgCl)/ WO_3 -FTO), WO_3 films grown on FTO substrate was used as working electrode; platinum and Ag/AgCl electrode were used as counter and reference electrodes, respectively. 0.5M Na_2SO_4 aqueous solution was taken as electrolyte.

3. Results and discussion

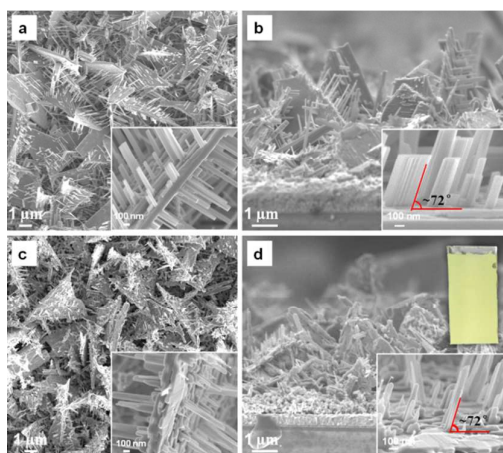


Fig.1 Top-view and Cross-sectional view SEM images of as-prepared hierarchical $\text{WO}_3(\text{H}_2\text{O})_x$ (a, b) and W500 (c, d) samples. The digital picture of W500 sample (2 cm \times 4 cm) is shown in the up right corner of (d).

Fig.1a-d show the SEM top-views and cross-views of the as-prepared hierarchical $\text{WO}_3(\text{H}_2\text{O})_x$ and its corresponding hierarchical WO_3 nanostructure (W500) after annealing at 500°C for 2h under air atmosphere. Clearly, the as-prepared $\text{WO}_3(\text{H}_2\text{O})_x$ hierarchical architectures were constructed of triangular sheet with side lengths of $\sim 6\text{-}7\mu\text{m}$ and thickness of $\sim 150\text{ nm}$ and flat plates with thickness of 20 nm and length of $\sim 100\text{-}500\text{ nm}$ as branches attached on the sheet with an angle of $\sim 72^\circ$ (the inset of Fig.1b). After calcinations, the smooth sheet surface turn rough and the flat sticks on the sheet were transformed to rods according to the magnified SEM images (the inset of Fig.1a and 1c), indicating a partial morphological change during the $\text{WO}_3(\text{H}_2\text{O})_x$ decomposition.

The hierarchical morphology was further analyzed by TEM. Fig.2a shows a low-magnification transmission electron microscopy (TEM) image of an as-prepared $\text{WO}_3(\text{H}_2\text{O})_x$ flake, which demonstrated a typical hierarchical architectures consisted of triangular sheet and flat sticks attached on the sheet, forming an integrated nanorod-nanosheet structure. Close TEM observation (Fig.2b) of sheet edge (marked with rectangle **b** in Fig.2a) reveals that the sheet was constructed from parallel aggregated nanorods with diameter of $\sim 15\text{ nm}$. The HR-TEM analyses were carried out on the flat stick (marked with rectangle **c** in Fig.2a) and the nanorod at the edge region of sheet (marked with rectangle **d** in Fig.2b) as shown in Fig.2c and Fig.2d respectively. A fringe spacing of 0.238 nm can be attributed to (240) lattice plane in the flat stick. The (002) lattice crystal plane with a fringe spacing of

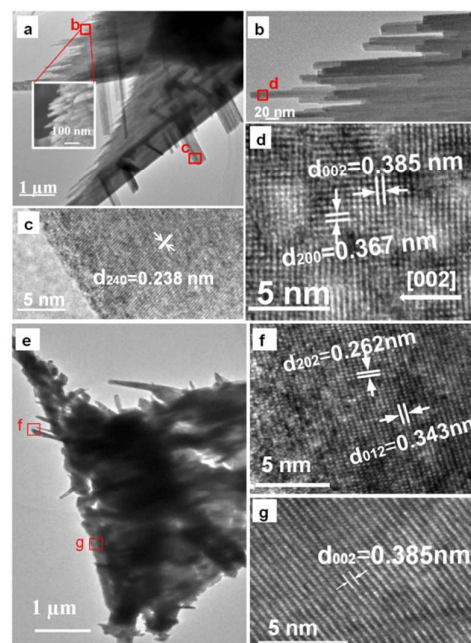


Fig.2 Low-magnification TEM images (a and e) and high-resolution TEM images (b, c, d, f and g) of the pristine hierarchical $\text{WO}_3(\text{H}_2\text{O})_x$ and W500 sample.

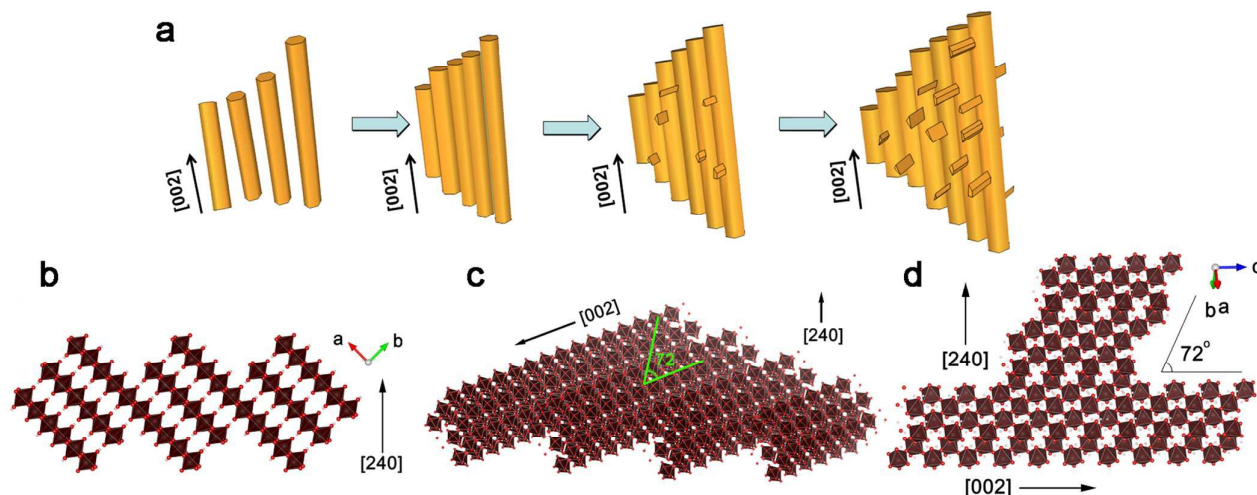


Fig.3 Schematic illustration of (a) self-assembly growth process of sheet-like hierarchical hydrated tungsten trioxide; (b) view from c-axis showing how the nanorods binding together; (c) profile atomic model of nanosheet; (d) profile atomic model of flat sticks as branches standing on the nanosheet.

0.385 nm indicates its growth direction along [002] for each single rod in the nanosheets. Fig.2e shows the TEM image of the obtained hierarchical WO_3 nanostructures. It can be found that the surface of the sheet became rugged and porous which could be a result of dehydration and aggregation of nanorods during process of calcinations. The high-resolution TEM images in Fig.2f and Fig.2g revealed different crystallographic plane orientations for the nanorod and sheet with lattice fringe of 0.262nm (202), 0.343nm (012) and 0.385 (002), indicating a polycrystalline nature of hierarchical WO_3 structure with high crystalline quality.

The plausible formation process of hierarchical $\text{WO}_3(\text{H}_2\text{O})_x$ structure is shown schematically in Fig.3a. The beginning is nucleating and initial growth of aligned nanorods along [002]. Further growth of more nanorods induces a subsequent binding of nanorods, result in the formation of a sheet-like

architecture. Fig.3b showed the atomic model for how the nanorods binding together with a view from c-axis. Upon the nanosheet flat sticks as branches grew along the [240] direction, forming a typical angle of 72° between the nanosheet and flat stick, as shown in Fig. 3d. The exposed facet of the nanosheets and flat sticks are (240) and (114) facet, respectively.

To further confirm the structure of the as-synthesized pristine sample and corresponding hierarchical WO_3 nanostructures after annealing, X-ray diffraction (XRD) patterns were conducted and shown in Fig.4. All the peaks of the pattern shown in the lower part of Fig.4 could be indexed to the orthorhombic phase of tungsten trioxide hydrate (JCPDS 01-072-0199, $a=7.3590$, $b=12.5130$, $c=7.7040$) and a

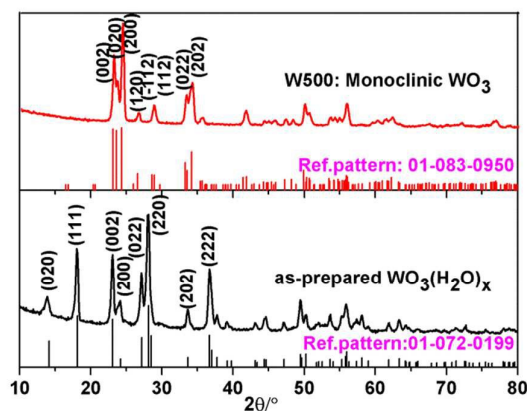


Fig.4 XRD patterns of the as-prepared hierarchical $\text{WO}_3(\text{H}_2\text{O})_x$ and W500 samples.

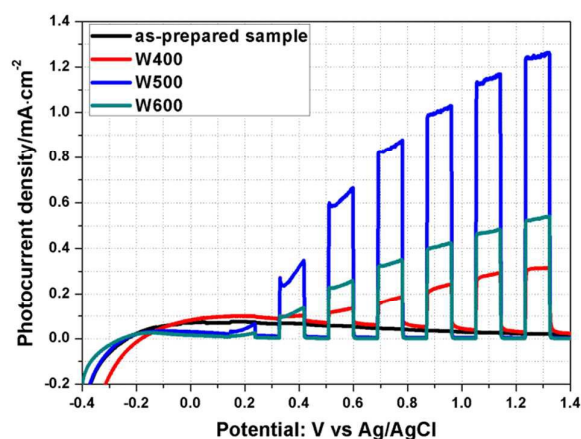


Fig.5 The photoelectrochemical performance of the as-prepared hierarchical $\text{WO}_3(\text{H}_2\text{O})_x$ sample and the obtained W400, W500 and W600 samples.

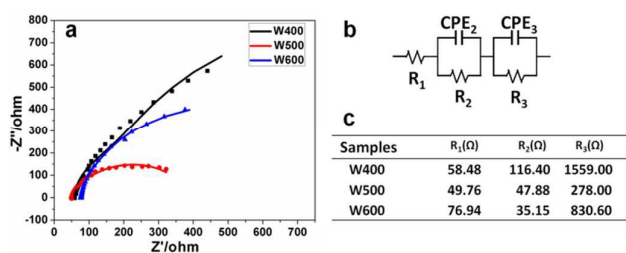


Fig.6 Electrochemical impedance spectroscopy of the WO_3 photoanodes measured at 0.5 V (vs. Ag/AgCl) in 0.5 M Na_2SO_4 solution. (a) Nyquist plots of the measured (plot) and fitted (line) impedance spectra. (b) The equivalent circuit for the photoanodes. (c) The fitted values of EIS parameters derived using the equivalent circuit model.

monoclinic structure (JCPDS 01-083-0950, $a=7.3008$, $b=7.5389$, $c=7.6896$, $\beta=90.8920^\circ$) was obtained after annealing the as-prepared sample at 500 °C, which was shown in the upper part of Fig.4. The TG-DSC plot recorded for the as-prepared hierarchical $\text{WO}_3(\text{H}_2\text{O})_x$ under air atmosphere at a heating rate of 10°C/min was shown in Fig.S1. The first weight loss of ~1.2% at around 300 °C is attributed to the loss of structural water in the WO_3 hydrate. Two following sharp weight losses of ~1.6% and ~1.0% at range 300 from 440°C and 440 from 500°C, respectively, with a increasing velocity could be due to the departure of residual NH_4^+ incorporated in the $\text{WO}_3(\text{H}_2\text{O})_x$ phase, and further release of H_2O .

To further investigate the influence of annealing temperature on the phase transformation of hydrated tungsten oxide and their photoelectrochemical performance, XRD, Raman spectra and electrochemical impedance spectroscopy (EIS) behaviours for samples obtained by annealing the as-prepared hydrated tungsten oxide at different temperatures were measured. Different from that annealed at 500°C, a lower annealing temperature of 400°C resulted in a hexagonal (*h*- WO_3) phase with the same hierarchical structures as the unannealed sample and a higher temperature of 600°C gives a monoclinic (*m*- WO_3) phase and a morphology of WO_3 sheet with branches collapsed, as shown in Fig.S2 and Fig.S3. The Raman spectroscopy of as-prepared $\text{WO}_3(\text{H}_2\text{O})_x$ and the obtained hexagonal and monoclinic WO_3 annealed at different temperature were performed and shown in Fig.S4. The weak peaks at 686, 796 and 912 cm^{-1} for the as-prepared sample can attributed to the characteristic peaks of $\text{WO}_3(\text{H}_2\text{O})_x$. After calcinations at 400°C, clear peaks at 248, 686 and 812 cm^{-1} were observed, which indicating a hexagonal WO_3 phase. With the increase of annealing temperature to 500°C and 600°C, characteristic peaks for the monoclinic WO_3 phase²⁴ at 128, 267, 321, 713 and 802 cm^{-1} were observed.

Fig.5 displays the photoelectrochemical performance of the as-prepared hierarchical sample and W400, W500 and W600 samples obtained by annealing at different temperatures: 400°C, 500°C and 600°C, respectively. There is no photocurrent response for the as-prepared $\text{WO}_3(\text{H}_2\text{O})_x$ and photocurrent response are significantly enhanced after annealing. The monoclinic WO_3 showed a better PEC activity

than that of hexagonal WO_3 obtained by annealing temperature of 400°C. The highest photocurrent density of 1.25 mA/cm^2 at 1.3V versus Ag/AgCl was obtained for 500°C calcination sample (W500). Electrochemical impedance spectroscopy (EIS) measurements were carried out to study the interface charge transport behaviour for the obtained WO_3 nanostructures (Fig.6). A smaller arc radius under illumination was found for the sample W500 as compared to the W400 and W600 (Fig.6a), indicating a fast interfacial charge transfer and this is in accordance with different photocurrent performances of the three samples. Which reflected by the minimum fitted values of R (Fig.6c) calculated using the equivalent circuit model shown in Fig.6b.

The growth behaviour of the hierarchical $\text{WO}_3(\text{H}_2\text{O})_x$ and corresponding WO_3 was influenced by the experimental parameters used. Two of the most important factors for formation of hierarchical structures were found to be the acidity of precursor solution and the amount of capping agent in precursor solution. Fig.S5 shows the SEM images the WO_3 samples obtained with different volumes (2ml-8ml) of concentrated hydrochloric acid added in the precursor and all the samples have been annealed with 500°C under air condition. It can be seen that only the sample synthesized with 4ml HCl solution added possesses hierarchical architectures composed of sheet and nanorods as branches. With 2ml HCl solution added in the precursor, nanograins with diameter of ~150nm were grown. While with 6ml or 8ml HCl solution added, small double-layer nanoflakes array with width of 500nm and thickness of 100nm were formed. All of these three types of WO_3 structure showed a lower photocurrent compared to the hierarchical WO_3 grown with 4ml HCl solution added as shown in Fig.S6. The amount of capping agent in precursor has been adjusted to disclose the effect of capping agent amount on the morphology of the obtained WO_3 structures. Fig.S7 shows the SEM images the WO_3 samples obtained with different amount of capping agent of (a) 0.5mmol, (b) 1.0mmol, (c) 2.0mmol or (d) 3.0mmol added in the precursor. (All the samples have been annealed with 500°C under air condition). It was found that only with 2.0mmol capping agent added into the precursor hierarchical WO_3 structure can be obtained. When the capping agent was increased to 3.0mmol, irregular WO_3 wires/flakes were deposited. Notably, when with 1.0mmol or 0.5mmol capping agent was added in precursor for solvothermal synthesis, rod-like WO_3 array was fabricated. The PEC performance shown in Fig.S8 indicated that similar photocurrents were obtained for samples with more than 0.5mmol capping agent added in the precursor.

4. Conclusions

In summary, a novel hierarchical $\text{WO}_3(\text{H}_2\text{O})_x$ structure, constructed with nanosheet as stem and plate-like nanorods as branches, was synthesized with a simple solvothermal method. Detailed investigation of its structural and morphological properties indicates that the growth mechanism is a self-assembly attachment process of fine

nanorods onto nanosheets along [240] direction. With a heating treatment under air atmosphere, preserved triangular hierarchical WO₃ structures were obtained. Annealing at different temperatures was carried out to witness a phase transformation from orthorhombic tungsten trioxide hydrate to hexagonal WO₃ at 400°C and finally to monoclinic WO₃ at 500°C. The experimental parameters of acidity of precursor and amount of capping agent added in the precursor were found exerting a strong effect on the growth of hierarchical WO₃ architectures.

Acknowledgements

This work was supported by the National Natural Science Foundation of China (No.51202186, No. 51236007).

Notes and references

- 1 A. Fujishima, K. Honda, *Nature*, 1972, **238**, 37.
- 2 I. S. Cho, Z. Chen, A. J. Forman, D. R. Kim, P. M. Rao, T. F. Jaramillo and X. Zheng, *Nano Lett.*, 2011, **11**, 4978.
- 3 N. Liu, C. Schneider, D. Freitag, M. Hartmann, U. Venkatesan, J. Müller, E. Spiecker and P. Schmuki, *Nano Lett.*, 2014, **14**, 3309.
- 4 M. Wang, J. Iocozzia, L. Sun, C. Lin and Z. Lin, *Energy Environ. Sci.*, 2014, **7**, 2182.
- 5 K. Mahmood, B. S. Swain and A. Amassian, *Adv. Mater.*, 2015, **27**, 2859.
- 6 H. Bai, Z. Liu and D. D. Sun, *Chem. Commun.*, 2010, **46**, 6542.
- 7 F. Nunzi, L. Storchi, M. Manca, R. Giannuzzi, G. Gigli and F. D. Angeli, *ACS Appl. Mater. Interfaces*, 2014, **6**, 2471.
- 8 H. Kim and K. Yong, *Phys. Chem. Chem. Phys.*, 2013, **15**, 2109.
- 9 Z. Li, Y. Ding, Y. Xiong, Q. Yang and Y. Xie, *Chem. Commun.*, 2005(7), 918.
- 10 J. Zhu, Z. Yin, D. Yang, T. Sun, H. Yu, H. E. Hoster, H. H. Hng, H. Zhang and Q. Yan, *Energy Environ. Sci.*, 2013, **6**, 987.
- 11 C. Zhang, X. Zhang, Y. Wang, S. Xie, Y. Liu, X. Lu and Y. Tong, *New J. Chem.*, 2014, **38**, 2581.
- 12 Y. Qiu, G. Xu, Q. Kuang, S. Sun, and S. Yang, *Nano Res.*, 2012, **5**, 826.
- 13 S. Guo, M. Zhen, M. Sun, X. Zhang, Y. Zhao and L. Liu, *RSC Adv.*, 2015, **5**, 16376.
- 14 W. Zeng, Y. Li and H. Zhang, *J Mater Sci: Mater Electron*, 2014, **25**, 1512.
- 15 J. Li, X. Liu, J. Cui and J. Sun, *ACS Appl. Mater. Interfaces*, 2015, **7**, 10108.
- 16 Z. Yao, J. Di, Z. Yong, Z. Zhao and Q. Li, *Chem. Commun.*, 2012, **48**, 8252–8254.
- 17 Y. Baek, Y. Song and K. Yong, *Adv. Mater.*, 2006, **18**, 3105.
- 18 Y. Hou, F. Zuo, A. P. Dagg, J. Liu and P. Feng, *Adv. Mater.*, 2014, **26**, 5043
- 19 Z. Zheng, W. Xie, Z. S. Lim, L. You and J. Wang, *Sci. Rep.*, 2014, **4**, 5721; DOI:10.1038/srep05721.
- 20 F. Xu, M. Dai, Y. Lu and L. Sun, *J. Phys. Chem. C*, 2010, **114**, 2776.
- 21 D. Ma, J. Jiang, J. Huang, D. Yang, P. Cai, L. Zhang and S. Huang, *Chem. Commun.*, 2010, **46**, 4556.
- 22 S. Jia, H. Zheng, H. Sang, W. Zhang, H. Zhang, L. Liao and J. Wang, *ACS Appl. Mater. Interfaces*, 2013, **5**, 10346.
- 23 J. Su, L. Guo, N. Bao and C. A. Grimes, *Nano Lett.*, 2011, **11**, 1928.
- 24 A. J. E. Rettie, K. C. Klavetter, J. Lin, et al., *Chem. Mater.*, 2014, **26**, 1670.

Hierarchical Architecture of WO₃ Nanosheets by Self-assembly of Nanorods for Photoelectrochemical Application

Tao Zhang, Jinzhan Su* and Liejin Guo*

International Research Center for Renewable Energy, State Key Laboratory for Multiphase Flow in Power Engineering, Xi'an Jiaotong University, Xi'an 710049, P. R. China

E-mail: j.su@mail.xjtu.edu.cn, lj-guo@mail.xjtu.edu.cn.

A self-assembly of WO₃ nanorod-nanosheet hierarchical architecture was deposited on the FTO by a simple solvothermal growth route.

